Journal of Controlled Release 383 (2025) 113851

Contents lists available at ScienceDirect

Journal of Controlled Release

journal homepage: www.elsevier.com/locate/jconrel

In situ therapeutic vaccines for leukemia by chemo-nanoadjuvant therapy☆

Peng Zhang [a], Guanhong Cui [a], Tanzhen Wang [b], Xiaofei Zhao [a], Xinyue Wang [c], Ruonan Ye [a], Tianhui Liu [b,**], Yiran Zheng [c,**], Zhiyuan Zhong [a,c,*]

[a] *Biomedical Polymers Laboratory, College of Chemistry, Chemical Engineering and Materials Science, and State Key Laboratory of Radiation Medicine and Protection, Soochow University, Suzhou, 215123, PR China*

[b] *National Clinical Research Center for Hematologic Diseases, Jiangsu Institute of Hematology, The First Affiliated Hospital of Soochow University, Collaborative Innovation Center of Hematology, Soochow University, Suzhou 215000, PR China*

[c] *College of Pharmaceutical Sciences, Soochow University, Suzhou 215123, PR China*

ARTICLE INFO

Keywords:
Cancer vaccines
Blood cancer
Nanoadjuvants
Polymersomes
Immunogenic cell death

ABSTRACT

Therapeutic vaccines introduce a potentially ultimate cure for cancers including leukemia. The personalized vaccines relying on neoantigens though exhibiting clinical benefits are afflicted by long and delicate manufacture procedure, high cost, and possibly incomplete coverage of heterogeneous tumor cells. Here, we report a facile strategy to generate potent *in situ* therapeutic vaccines, which effectively eliminate leukemia and induce long-term anti-leukemia immunity, by homoharringtonine-nano-dual-adjuvant (HHT-NDA) therapy. HHT effectively kills leukemia cells and generates abundant tumor antigens *via* inducing immunogenic cell death. NDAs cooperatively promote the maturation and antigen-presentation of dendritic cells by activating both nucleotide-binding oligomerization domain-containing protein 2 and toll-like receptor 9. The HHT-NDA treatment of murine MLL-AF9 acute myeloid leukemia model leads to 57–71 % complete regression and 100 % protection from rechallenge, in accordance with expansion of memory $CD8^+$ T cells. This standard-of-care chemotherapy in tandem with nano-dual-adjuvant offers a novel strategy to generate *in situ* therapeutic vaccines for leukemia.

1. Introduction

Therapeutic cancer vaccines have demonstrated promising potential in early clinical trials [1–3]. To effectively elicit robust and sustained immune responses against tumor cells, these vaccines require both tumor antigens (Ags) and immunostimulatory adjuvants as essential components [4]. Tumor heterogeneity and the scarcity of shared tumor Ags have significantly heightened interest in personalized cancer vaccines [5]. Neoantigens, which arise exclusively from somatic mutations in cancer cells and are uniquely expressed by tumor cells, have enabled personalized vaccines to achieve clinical benefits [1,2]. However, further development of these vaccines faces substantial challenges, including the limited chance of identifying immunogenic neoantigens, time-consuming manufacturing processes, technical complexity, high cost, and potentially incomplete coverage of heterogeneous tumor cells [6,7]. In contrast, employing tumor cell lysate, tumor cell components or whole tumor cells as Ag sources can bypass the need for identifying and synthesizing neoantigens [8,9]. Nevertheless, challenges persist in acquiring sufficient tumor cells for vaccine production and ensuring stringent quality control [10,11].

In situ cancer vaccines can circumvent these issues by generating Ags from tumors *in vivo* [12]. To treat solid tumors, various strategies including chemotherapy, radiotherapy, photodynamic therapy, photothermal therapy, or their combinatorial approaches have been employed to trigger immunogenic cell death (ICD) of tumor cells, thereby facilitating Ag production [13–19]. ICD can also induce damage-associated molecular patterns (DAMPs) on tumor cells to enhance adjuvanticity [20]. However, ICD as a standalone approach often fails to elicit robust and durable anti-tumor immunity [21]. Additional adjuvants are often required to augment the potency of *in situ* cancer vaccines by stimulatng dendritic cells (DCs) and subsequently activating cytotoxic T lymphocytes (CTLs) [22,23]. Despite the development of *in situ* vaccines for solid tumor treatment, reports on hematologic malignancies (HM) are rare. Acute myeloid leukemia (AML) is one of the most aggressive,

☆ This article is part of a Special issue entitled: 'ESCDD2024' published in Journal of Controlled Release.

* Corresponding author at: Biomedical Polymers Laboratory, College of Chemistry, Chemical Engineering and Materials Science, and State Key Laboratory of Radiation Medicine and Protection, Soochow University, Suzhou, 215123, PR China.

** Corresponding authors.

E-mail addresses: liutianhui@suda.edu.cn (T. Liu), yrzheng@suda.edu.cn (Y. Zheng), zyzhong@suda.edu.cn (Z. Zhong).

https://doi.org/10.1016/j.jconrel.2025.113851
Received 13 December 2024; Received in revised form 25 April 2025; Accepted 14 May 2025
Available online 17 May 2025

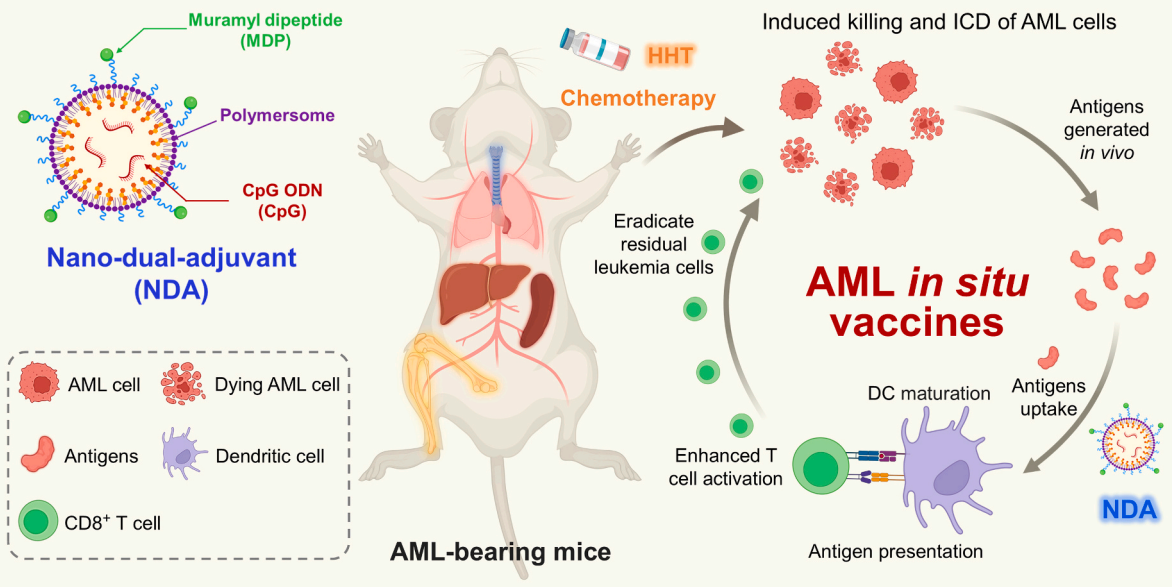

Scheme 1. Schematic illustration of NDA structure and *in situ* therapeutic vaccine HHT-NDA for AML treatment. NDAs with CpG in the core and MDP on the surface are formed by co-self-assembly of PEG-P(TMC-DTC)-SP and MDP-PEG-P(TMC-DTC) in the presence of CpG. HHT chemotherapy reduces leukemia burden and generates tumor Ags *in vivo*. NDAs activate NOD2 and TLR9 dual signaling pathway to induce anti-AML immunity for removal of residual leukemia cells and prevention of recurrence. HHT: homoharringtonine; NDA: nano-dual-adjuvant; DC: dendritic cell. Illustration was created in Biorender.com.

intractable and heterogeneous type of HM [24,25]. The 5-year survival rate of AML is only 30–50 % in adults, dropping to 7 % in patients over 65 years old [26]. The development of therapeutic vaccines against AML has been impeded by the absence of leukemia-specific neoantigens and the pronounced heterogeneity of AML cells [27]. We recently developed potent anti-AML vaccines by loading AML cell lysates and CpG into chimeric polymersomes formed from poly(ethylene glycol)-b-poly(trimethylene carbonate-co-dithiolane trimethylene carbonate)-b-spermine (PEG-P(TMC-DTC)-SP) and muramyl dipeptide (MDP)-functionalized PEG-P(TMC-DTC) [28]. These personalized vaccines, however, need to be customized for each individual, which is associated with long processing time, high cost and difficulty in quality control.

The chemotherapeutic agent homoharringtonine (HHT), a plant-derived alkaloid, has been used extensively to treat HM especially leukemia for over 40 years in China. Its efficacy was confirmed in multiple clinical trials in the United States [29–31]. A semisynthetic derivative of HHT, omacetaxine, has been approved by the US FDA for the treatment of chronic myeloid leukemia (CML) [32]. HHT is a potent inhibitor of protein translation and has demonstrated efficacy against leukemia cells harboring mutations in genes such as *FLT3, KIT, BCR-ABL1, RUNX1* and *BCL2*, which cover a substantial portion of AML cells [33–36]. Therefore, HHT can facilitate the generation of diverse leukemia Ags that might address the heterogeneity issue of AML.

Here we report a facile strategy to generate potent *in situ* therapeutic vaccines for AML through the sequential application of HHT chemotherapy and nano-dual-adjuvants (NDAs) (Scheme 1). NDAs, formed by encapsulating CpG into polymersomes co-self-assembled from PEG-P(TMC-DTC)-SP and MDP-PEG-P(TMC-DTC), are able to activate both nucleotide-binding oligomerization domain-containing protein 2 (NOD2) and Toll-like receptor 9 (TLR9) signaling pathways. HHT effectively eliminates leukemia cells, reducing tumor burden and generating leukemia Ags *in vivo*. NDAs stimulate Ag-specific and long-term anti-AML immunity, facilitating the clearance of residual leukemia cells and promoting immune memory generation to prevent recurrence. Unlike personalized vaccines, *in situ* anti-AML vaccines are robust and can be applied for different entities. Remarkably, HHT-NDA therapy achieved 57–71 % complete regression of murine AML and provided 100 % protection against leukemia cell rechallenge. HHT-NDA therapy provides an appealing strategy for generating *in situ* therapeutic vaccines for leukemia.

2. Materials and methods

2.1. Materials

CpG ODN 1826 (CpG, 5'-TCCATGACGTTCCTGACGTT-3') and Cy3-labeled CpG (CpG^{Cy3}) were purchased from Sangon Biotech. Muramyl dipeptide (MDP, Synpeptide Co.,Ltd.), ovalbumin (OVA, Sigma-Aldrich), GM-CSF (TargetMol), Homoharringtonine (HHT, purity: 99.75 %, MedChemExpress), D-Luciferin potassium salt (99 %, Bridgen Co., Ltd.), Cell Counting Kit-8 (CCK-8, Suzhou Fcmacs Biotech Co., Ltd.), and Annexin V-APC/7-AAD apoptosis detection kit (MultiSciences Biotech Co., Ltd) were used as received. Zombie NIR™ Fixable Viability Kit (Biolegend), Enhanced ATP Assay Kit (Beyotime Biotechnology), Mouse enzyme-linked immuno sorbent assay kits (ELISA kits, Invitrogen) for tumor necrosis factor alpha (TNF-α), interferon gamma (IFN-γ), interleukin 6 (IL-6), interleukin 1 beta (IL-1β) and high mobility group box 1 (HMGB-1 ELISA kits, Solarbio) were used as indicated by the manual. Antibodies (Abs) used for flow cytometry analysis are listed in **Table S1**.

2.2. Animals, cells and AML models

C57BL/6 mice and Balb/c mice (6-week-old, female) were purchased from Beijing Vital River Laboratory Animal Technology and Shanghai Jihui Laboratory Animal Care, respectively. Mice were housed in pathogen-free conditions at the Soochow University and all animal experiments were approved by the Animal Care and Use Committee of Soochow University. All protocols of animal studies were conformed to the Guide for the Care and Use of Laboratory Animals (approval number: 202308A0034, 202310A0238).

GFP^+ MLL-AF9 primary AML cells and WEHI-3-Luc AML cell line were obtained from the First Affiliated Hospital of Soochow University. Bone marrow-derived dendritic cells (BMDCs) were isolated from healthy C57BL/6 mice and were activated with GM-CSF for 7 days. MLL-AF9 AML model was established by intravenous (*i.v.*) infusion of 5×10^5 GFP^+ MLL-AF9 cells into C57BL/6 mice *via* tail vein. WEHI-3 AML model was established by *i.v.* infusion of 5×10^6 WEHI-3-Luc cells into

Balb/c mice *via* tail vein as previously described [28].

2.3. Preparation of NDA

Polymer PEG-P(TMC-DTC)-SP and MDP-PEG-P(TMC-DTC) were synthesized as previously reported [28,37]. Briefly, Two polymers (40 mg/mL) were mixed at a 1:1.2 M ratio in 100 μL DMF before addition to HEPES buffer (900 μL, 5 mM, pH 6.8) containing CpG at 4 wt% of polymer. The resulting mixture was dialyzed against membrane with MWCO at 1000 kDa in HEPES buffer for 3 h and then Phosphate Buffer (10 mM, pH 7.4) for another 3 h with fresh medium exchanged every hour.

2.4. Cytotoxicity, apoptosis and ICD induced by HHT

MLL-AF9 and WEHI-3-Luc cells were seeded at 2×10^4 cells/well while B16-OVA cells were at 4×10^3 cells/well in 96-well plates overnight for cytotoxicity test. Cells were then incubated with HHT (final concentration: 0.1–1000 nM) for 1 day before viability evaluation *via* a Cell Counting Kit-8 (CCK-8) following the manufacturer's instruction. Absorbance at 450 nm of each well was measured by a microplate reader (Thermo Scientific, USA).

The pro-apoptotic activity of HHT in MLL-AF9 cells was investigated using an Annexin V-APC/7-AAD apoptosis detection kit. Cells seeded in 12-well plates (2×10^5 cells/well) were treated with HHT (Concentration: 5 nM or 15 nM) for 1 day. Cells were then harvested, washed with cold saline, resuspended and stained with Annexin V-APC and 7-AAD for 5 min at 25 °C before evaluation by a flow cytometer (FACS Calibur, BD Biosciences, USA).

The ICD effect induced by HHT in MLL-AF9 cells was tested as follows: MLL-AF9 cells seeded in 12-well plates (2×10^5 cells/well) were treated with saline or HHT (5 nM and 15 nM) for 24 h. Then the amount of HMGB-1 and ATP in the supernatant was quantified by ELISA kit and ATP assay kit, respectively, by following manufacturer's instruction. The cells were stained by anti-CRT primary Ab and then Alexa fluor 633-conjugated secondary Ab for 20 min at 4 °C before flow cytometry analysis.

2.5. Maturation and ag presentation by BMDCs in vitro

BMDCs were seeded in 12-well plate (5×10^5 cells/well) and then incubated with saline, HHT, MLL-AF9 cells or HHT-treated MLL-AF9 cells (HHT Concentration: 5 nM) for 1 day ($n = 4$). BMDCs were then stained with anti-CD11c-PE-Cy7, anti-CD80-APC and anti-CD86-PE before flow cytometry analysis.

According to the design [38], HHT-treated MLL-AF9 cells were collected 24 h later and incubated with BMDCs, nanoadjuvants containing only MDP (NM) or CpG (NC), NDA or mixture of free dual adjuvants MDP/CpG (free DA) were then added and continuously incubated for 1 day ($n = 4$). The concentration of MDP and CpG used was at 0.25 μg/mL and 1 μg/mL, respectively. Pro-inflammatory cytokines (TNF-α, IL-6, IL-1β) in supernatants were quantified by using ELISA kits. To evaluate the Ag presentation ability by BMDCs, HHT-treated B16-OVA cells (HHT concentration: 5 nM) or OVA protein with/without NDA were incubated with BMDCs for 24 h (n = 4). Then BMDCs were stained with anti-CD11c-PE-Cy7 and anti-SIINFEKL H-2K^b-PE before flow cytometry analysis.

2.6. In vivo biodistribution and immune cell analysis

In vivo biodistribution of free CpG^{Cy3} and NDA loading with CpG^{Cy3} (NDA-CpG^{Cy3}) was studied in mice bearing with MLL-AF9 leukemia ($n = 3$). Formulations containing CpG (0.5 mg/kg) in 200 μL saline were injected *via* tail veins. Heart, liver, spleen, lung, kidney, femur + tibia (for bone marrow, BM) and inguinal lymph nodes (LNs) were dissected at 8 h post injection and Cy3 fluorescence was measured by *In Vivo* Imaging System (IVIS, PerkinElmer).

MLL-AF9 leukemia-bearing mice were randomly grouped on day 3 ($n = 5$). For combination therapy, mice were first treated with HHT intraperitoneally (*i.p.*) at 1 mg/kg to generate Ags *in vivo* and then *i.v.* injection of different formulations of nanoadjuvants (NM, NC or NDA) 10 h later to boost the subsequent immune response. [39] The dose for HHT, MDP and CpG each time was 1 mg/kg, 0.25 mg/kg and 1 mg/kg, respectively. Mice treated with saline or HHT alone served as control groups. All treatment were repeated for a total 5 times on day 3, 6, 9, 16 and 23 post leukemia cells transplantation. At 48 h after the last injection, peripheral blood (PB), LNs, and BM were harvested and processed into single cell suspensions. Before surface staining, the samples were sequentially incubated with Zombie NIR viability dye and Fc Block. To evalute maturation of DCs in LNs, cells were stained with anti-CD45-PerCP-Cy5.5, anti-CD11c-PE-Cy7, anti-CD80-APC and anti-CD86-PE. To evaluate CD8$^+$ T cells in PB and BM, cells were stained with anti-CD45-PerCP-Cy5.5, anti-CD3-APC, anti-CD4-PE and anti-CD8a-PE-Cy7. To evaluate Tregs in BM, cells were stained with anti-CD45-PerCP-Cy5.5 and anti-CD4-PE before fixation, permeabilization and staining with intracellular anti-Foxp3-Alexa Fluor 647. All samples were analyzed by flow cytometry. The concentration of IL-1β, IL-6, TNF-α and IFN-γ in serum was determined by ELISA kits.

2.7. Anti-AML efficacy of HHT-NDA in murine MLL-AF9 model

MLL-AF9 leukemia-bearing mice were randomly sorted into 7 groups on day 3 ($n = 7$) after inoculation with MLL-AF9 leukemia cells. For combination therapy, mice were first treated with HHT (*i.p.*) and 10 h later injection (*i.v.*) with different formulations of adjuvants (NM, NC, NDA or free DA). Control groups included saline, HHT-only, and NDA-only treatments. Doses were standardized at 1 mg/kg HHT, 0.25 mg/kg MDP, and 1 mg/kg CpG per administration, delivered on day 3, 6, 9, 16, and 23 post-transplantation. PB (~50 μL) was collected retro-orbitally from each mouse at regular intervals. Harvested PB was then treated with ACK lysis buffer for 10 min to remove red blood cells and the percentage of GFP$^+$ AML cells in PB was quantified *via* flow cytometry. Evaluation of the efficacy of HHT-NDA for AML at advanced stages, the initial treatment starts on day 6. Mice treated with saline or HHT were served as controls. The percentages of GFP$^+$ AML cells in PB were quantified as described above.

For leukemia burden analysis, MLL-AF9-bearing mice were divided into 5 groups on day 3 ($n = 5$). For combination therapy, mice were treated with HHT (*i.p.*) and 10 h later injection (*i.v.*) with different formulations of adjuvants (NM, NC or NDA). The dosages of treatment were the same as above. After mice were sacrificed on day 25, PB, BM, spleen, liver and lung were harvested and processed into single cell suspensions. Percentages of GFP$^+$ AML cells in these tissues were analyzed *via* flow cytometer.

2.8. Evaluation of generated anti-AML immune memory

Cured mice ($n = 4$) were re-challenged with GFP$^+$ MLL-AF9 cells (5×10^5 cells per mouse). MLL-AF9-bearing mice and naive mice (healthy mice without leukemia transplantation) were served as positive and negative controls, respectively. PB was collected from each mouse at regular intervals until day 24 post re-challenge and the percentages of GFP$^+$ AML cells in were quantified as described above. All mice were sacrificed on day 24. Hind leg bones and spleens from each group were photographed for macroscopic evaluation and the weights of spleen and liver were recorded. The leukemia burden in BM, spleen, liver and lung were analyzed *via* flow cytometry. Moreover, CD8$^+$ effector memory T cells (T_{EM}, CD44$^+$CD62L$^-$) in spleen were also quantified by flow cytometry. Before surface staining, all spleen samples were incubated with Zombie NIR viability dye and Fc Block as described above. Then these samples were stained with anti-CD45-BV605, anti-CD3-APC, anti-CD8-PE-Cy7, anti-CD44-PerCP-Cy5.5 and anti-CD62L-BV421 before

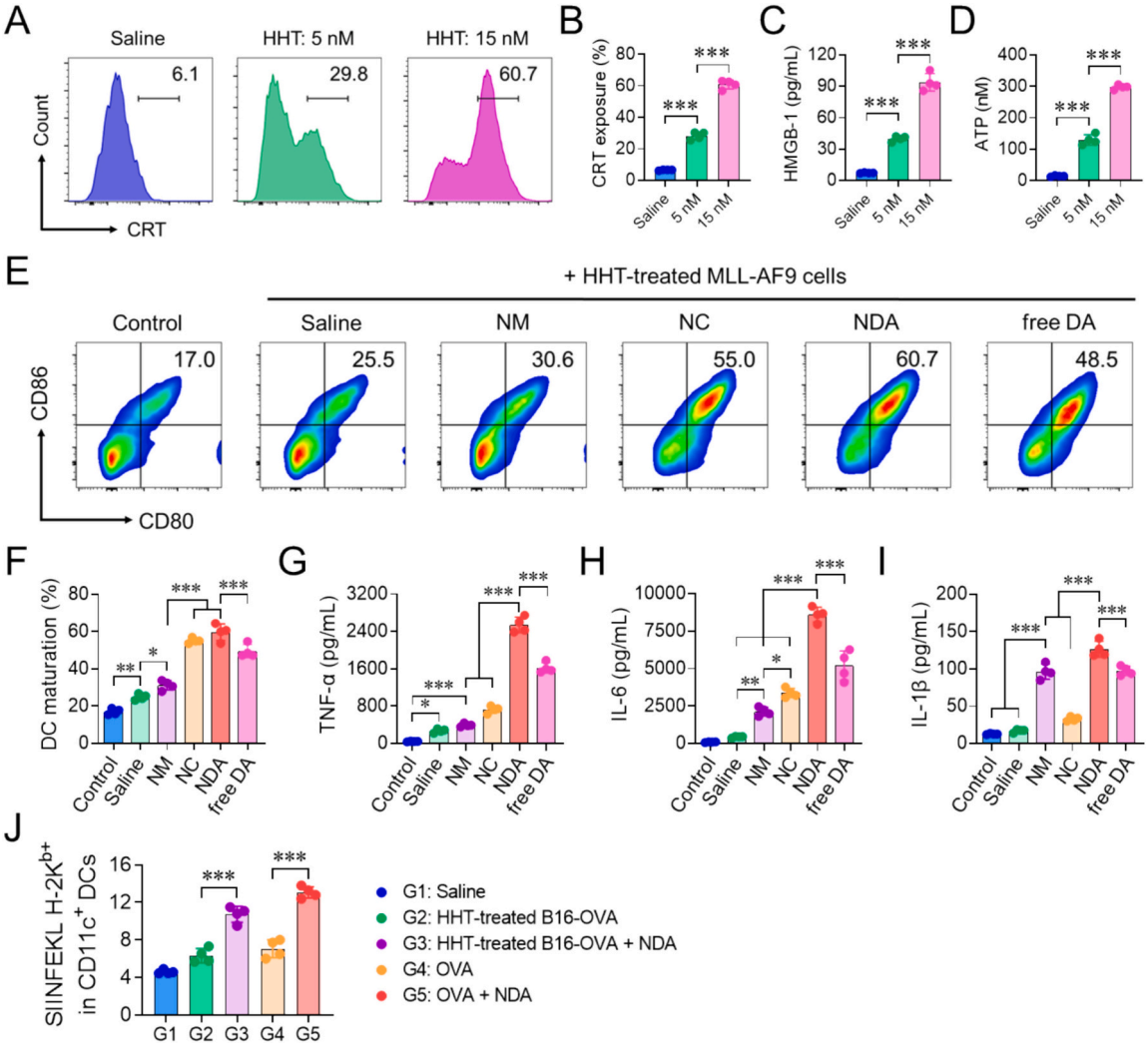

Fig. 1. HHT-NDA substantially promoted the BMDC maturation *in vitro*. (A-D) MLL-AF9 AML cells were treated with varying concentrations of HHT for 24 h before analysis. (A) Sample histogram and (B) quantitative analysis of cell-surface expression of calreticulin (CRT). Quantification of secreted (C) high mobility group box-1 (HMGB-1) and (D) ATP in culture media. (*E*-I) BMDCs were co-incubated with HHT-treated MLL-AF9 cells in conjunction with different formulations of adjuvants for 24 h before analysis. (E) Representative flow cytometry plots and (F) percentage of mature BMDCs ($CD80^{+}CD86^{+}$ cells in $CD11c^{+}$ cells). Amount of pro-inflammatory cytokine (G) TNF-α, (H) IL-6 and (I) IL-1β secreted by BMDCs. (J) Percentage of BMDCs expressing SIINFEKL H-$2k^{b}$ after co-incubating BMDCs with saline, OVA, OVA with NDA, HHT-treated B16-OVA cells, and HHT-treated B16-OVA cells with NDA. $n = 4$, data was compared by one-way ANOVA with Tukey's post test, $^{*}p < 0.05$, $^{**}p < 0.01$, $^{***}p < 0.001$.

analysis.

2.9. Anti-AML efficacy of HHT-NDA in murine WEHI-3-Luc model

WEHI-3-Luc-bearing mice were randomly divided into 3 groups on day 3 ($n = 7$). For combination therapy, mice were first treated with HHT (*i.p.*) and then intravenously infused with NDA 10 h later. Saline- and NDA-only groups served as controls. Doses were standardized at 1 mg/kg HHT, 0.25 mg/kg MDP, and 1 mg/kg CpG per administration, delivered on day 3, 6, 9, 16, and 23 post-transplantation. The whole-body bioluminescence signals from WEHI-3-Luc cells were monitored by IVIS for every 10 days. Each mouse was injected (*i.p.*) with D-Luciferin (75 mg/kg) and images were acquired 10 min post-injection. The bioluminescence signals were analyzed by Living Image 4.7.4 software.

2.10. Statistical analysis

The data were presented as mean ± SD and analyzed by Prism 8.1. Flow cytometry data was analyzed by FlowJo version 10. Comparisons between multiple groups were analyzed by one-way ANOVA with Tukey post-test unless otherwise indicated. Comparison between two groups were done by two-tailed paired Student *t*-test. Kaplan-Meier survival curves were analyzed by log-rank test. $^{*}p < 0.05$, $^{**}p < 0.01$, $^{***}p < 0.001$ and $^{****}p < 0.0001$.

3. Results and discussion

3.1. HHT-pretreated AML cells and NDAs robustly stimulate BMDCs in vitro

The development of *in situ* vaccines relies on the effective elimination of tumor cells for Ag production and the availability of potent immunostimulatory adjuvants. The chemotherapeutic agent HHT potently induced death of MLL-AF9 primary AML cells and WEHI-3 leukemia cell line through both apoptotic and necrotic pathways (**Fig. S1 A, B**). Notably, HHT elicited strong ICD, as evidenced by the upregulation of surface-exposed calreticulin (CRT) and elevated secretion of high mobility group box-1 (HMGB-1) and adenosine triphosphate (ATP) (Fig. 1A-D). These DAMP signals enhanced the stimulation of DCs. BMDCs co-cultured with HHT-treated MLL-AF9 cells exhibited

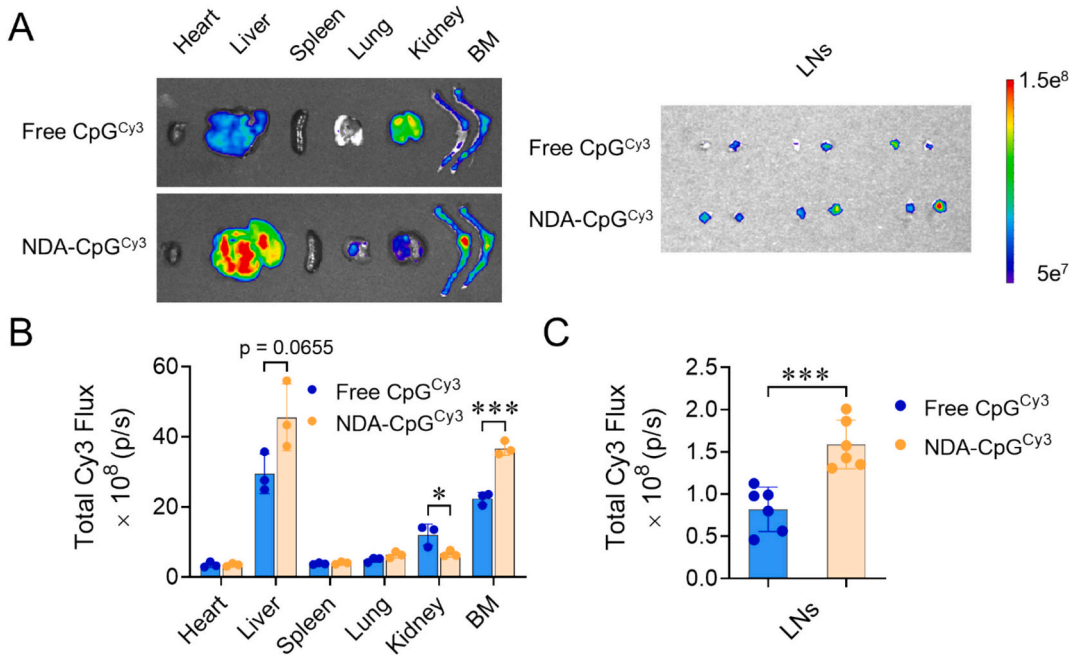

Fig. 2. NDAs enhanced the biodistribution of adjuvants in BM and LNs. MLL-AF9-bearing mice were *i.v.* injected with Cy3 labeled free CpG (Free CpG^{Cy3}) or CpG^{Cy3}-loaded NDA (NDA-CpG^{Cy3}). (A) IVIS images of Cy3 fluorescence in major organs. Semi-quantitative analysis of Cy3 fluorescent signals in heart, liver, spleen, lung, kidney, and BM (B), and in LNs (C). Statistical analysis was performed by student *t*-test for B and C, $*p < 0.05$, $***p < 0.001$.

significantly higher expression of CD80 and CD86 compared to those co-cultured with untreated cells (**Fig. S2**). Therefore, HHT treatment not only effectively generates tumor Ags, but also promotes DC maturation.

To synergize with HHT for generating potent *in situ* vaccines, we utilized NDAs to amplify anti-AML immune responses. We previously engineered a polymersome-based system to co-deliver exogenously prepared Ags and adjuvants for eliciting robust anti-leukemia immunity [28]. In the current study, we employed the nanosystem to co-deliver adjuvants MDP and CpG for simultaneous activation of NOD2 and TLR9 signaling pathways, enabling complementary activation of DCs [40]. The dual-action mechanism of NDAs combined with HHT-triggered ICD substantially enhanced DC activation. Nanoadjuvants NM or NC upregulated CD80 and CD86 expression on BMDCs while NDA induced the highest maturation rate of BMDCs (Fig. 1E, F). In addition, NDAs dramatically enhanced the secretion of proinflammatory cytokines by BMDCs than NM and NC. Specifically, NDAs induced 6.4 and 3.5-fold increases in tumor necrosis factor alpha (TNF-α), 4.0 and 2.6-fold increase in interleukin-6 (IL-6), and 1.3 and 3.8-fold increase in interleukin-1β (IL-1β), in comparison to the single adjuvant NM and NC, respectively (Fig. 1G-I). NDAs also outperformed the physical mixture of free MDP and CpG in inducing BMDC maturation and secretion of proinflammatory cytokines (Fig. 1G-I), demonstrating the critical role of the nanodelivery system. Moreover, when employing the model Ag OVA, NDAs significantly enhanced the Ag presentation ability of BMDCs. Given the absence of OVA-expressing AML cells, B16-OVA cells were treated by HHT to serve as the source of Ag OVA instead. NDA also improved the presentation of tumor-cell-derived OVA by BMDCs (Fig. 1J **and Fig. S3**).

Our results demonstrated that HHT can efficiently induce ICD in AML cells. Although ICD alone often fails to sufficiently activate the immune system *in vivo* [12], HHT-induced ICD synergizes with NDAs to amplify immunostimulation, thereby further promoting DC stimulation and Ag presentation [21,41].

3.2. HHT-NDA therapy generates potent and systemic anti-leukemia immunity in mice

We evaluated the biodistribution of free CpG^{Cy3} and NDA loaded with CpG^{Cy3} in mice post *i.v.* injection. The majority of free CpG was observed in the kidneys, indicative of renal clearance of CpG due to its small size (Fig. 2A, B). Compared with free CpG, NDA elicited a 1.6-fold and 1.9-fold increase in the fluorescence signal in BM and inguinal LNs, respectively (Fig. 2A-C), which suggests that NDA would induce systemic innate immune activation. HHT is typically administrated *via i.p.* injection and can effectively kill AML cells in PB and major organs, generating AML Ags throughout the body [25,42]. Hence, HHT-NDA therapy would likely invigorate adaptive, Ag-specific immune response.

To investigate the effects of HHT-NDA therapy on anti-leukemia immune responses, MLL-AF9-bearing mice were injected with HHT (*i.p.*). to generate Ags systemically *in vivo*, followed by *i.v.* administration of nanoadjuvants 10 h later. Five consecutive treatment cycles were administered and immune cells in LNs, PB and BM were analyzed two days after the last dose (Fig. 3A). The average percentages of mature ($CD80^+CD86^+$) DCs in inguinal LNs from the saline and HHT-only groups were lower than those in groups treated with HHT combined with single nanoadjuvants (HHT-NM and HHT-NC). The use of HHT combined with NDAs elicited the highest DC maturation level (Fig. 3B, C), demonstrating the superior efficacy of this combination in stimulating DCs within the inguinal LNs.

The presence of anti-tumor immunity in BM is often correlated with the treatment outcomes of AML, as AML originates from the myeloid progenitors within the BM microenvironment [43,44]. Following treatment with HHT-NDA, the proportion of $CD8^+$ T cells in the BM increased by at least 7-fold compared to saline and HHT-only controls (Fig. 3D, E). Moreover, HHT-NDA also elicited a higher proportion of $CD8^+$ T cells than HHT combined with NM or NC. Elevated regulatory T cells (Tregs) level in BM are associated with disease progression, and reducing Tregs in BM has shown promising efficacy in alleviating leukemic burden [45,46]. HHT-NDA reduced BM Treg proportions to 1/4 of that elicited by HHT-only treatment (Fig. 3F, G). Furthermore, the $CD8^+$ T/Treg ratio in BM increased to 4.1 post-HHT-NDA treatment as

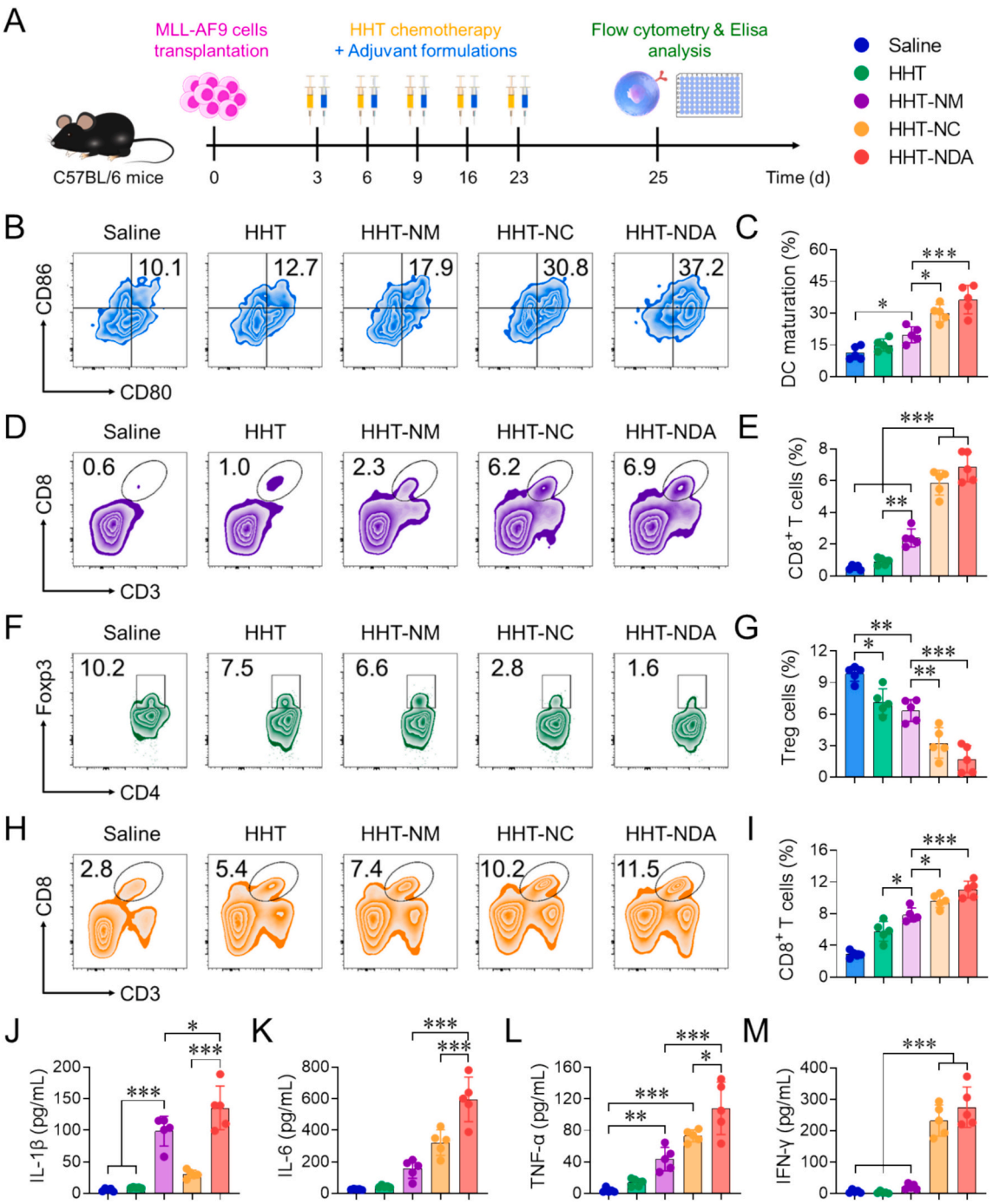

Fig. 3. HHT-NDA effectively elicited anti-AML immune responses in LNs, BM and PB. (A) Timeline for analyzing immune responses generated by different treatment strategies in murine MLL-AF9 AML model. (B) Representative flow cytometry plots and (C) percentage of matured ($CD80^+CD86^+$) DCs in inguinal LNs. (D) Representative flow cytometry plots and (E) average percentages of $CD8^+$ T cells in BM. (F) Representative flow cytometry plots and (G) average percentages of Tregs in BM. (H) Representative flow cytometry plots and (I) average percentages of $CD8^+$ T cells in PB. (F) Serum levels of pro-inflammatory cytokine (J) IL-1β, (K) IL-6, (L) TNF-α, and (M) IFN-γ. $n = 5$, comparison between multiple groups was done by one-way ANOVA, $^*p < 0.05$, $^{**}p < 0.01$, $^{***}p < 0.001$.

opposed to 0.05 in Saline controls, indicating the effective reversal of immunosuppression.

HHT-NDA treatment also elicited the highest percentage of $CD8^+$ T cells in PB, showing 3.8-fold increase from that of the Saline control (Fig. 3H, I). In addition, HHT-NDA dramatically enhanced the levels of multiple pro-inflammatory cytokines in serum (Fig. 3J-M). MDP preferentially induced IL-1β, whereas CpG predominantly elevated IL-6, IFN-γ and TNF-α [47]. Consistent with adjuvant-specific effects, HHT-NM substantially increased the secretion of IL-1β while HHT-NC boosted secretion of IL-6, TNF-α and IFN-γ (Fig. 3J-L). Notably, HHT-NDA elicited a significantly higher level of IL-1β than HHT-NM (Fig. 3J) as well as 1.9-fold higher IL-6, 1.5-fold higher TNF-α, and elevated IFN-γ compared to HHT-NC (Fig. 3K-M). These results demonstrated that engaging both NOD2 and TLR9 signaling pathways simultaneously elicit complementary stimulation compared to activating single pathway. Overall, it is evident that HHT-NDA elicited robust and systemic immune responses in leukemia-bearing mice.

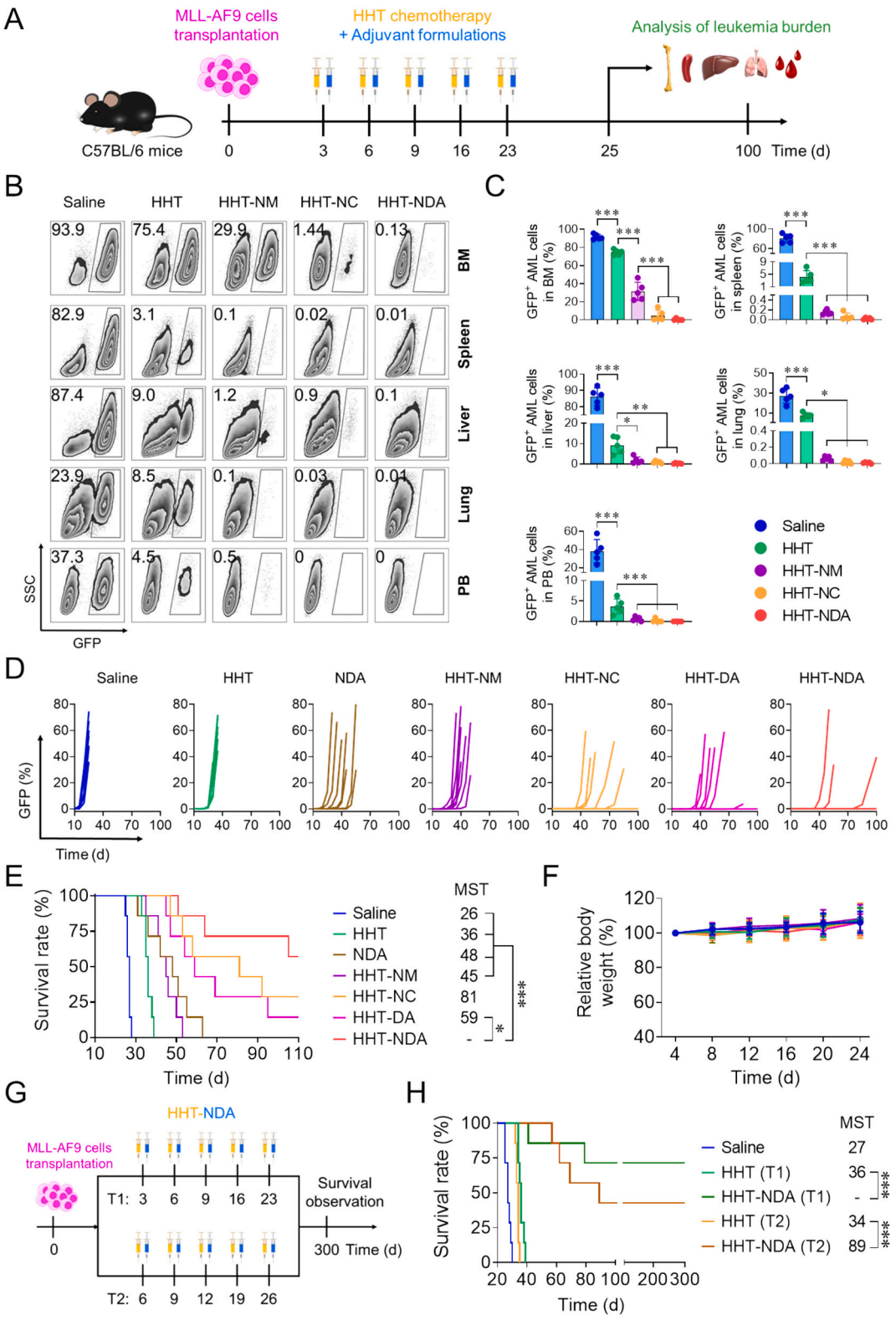

Fig. 4. HHT-NDA yielded remarkable efficacy in murine MLL-AF9 AML model. (A) Timeline for the therapy experiment. (B) Representative flow cytometry plots and (C) percentage of GFP$^+$ AML cells engraftment in PB and major organs of mice on day 25 ($n = 5$). (D) Percentage of GFP$^+$ AML cells in PB at different time points ($n = 7$). (E) Survival curve (n = 7). (F) Body weight of mice following different treatments (n = 7). (G) Timeline for therapy experiment treating advanced stage of AML. (H) Survival curve (n = 7). Log-rank test conducted for E, H and one-way ANOVA analysis was performed for C, $^*p < 0.05$, $^{**}p < 0.01$, $^{***}p < 0.001$.

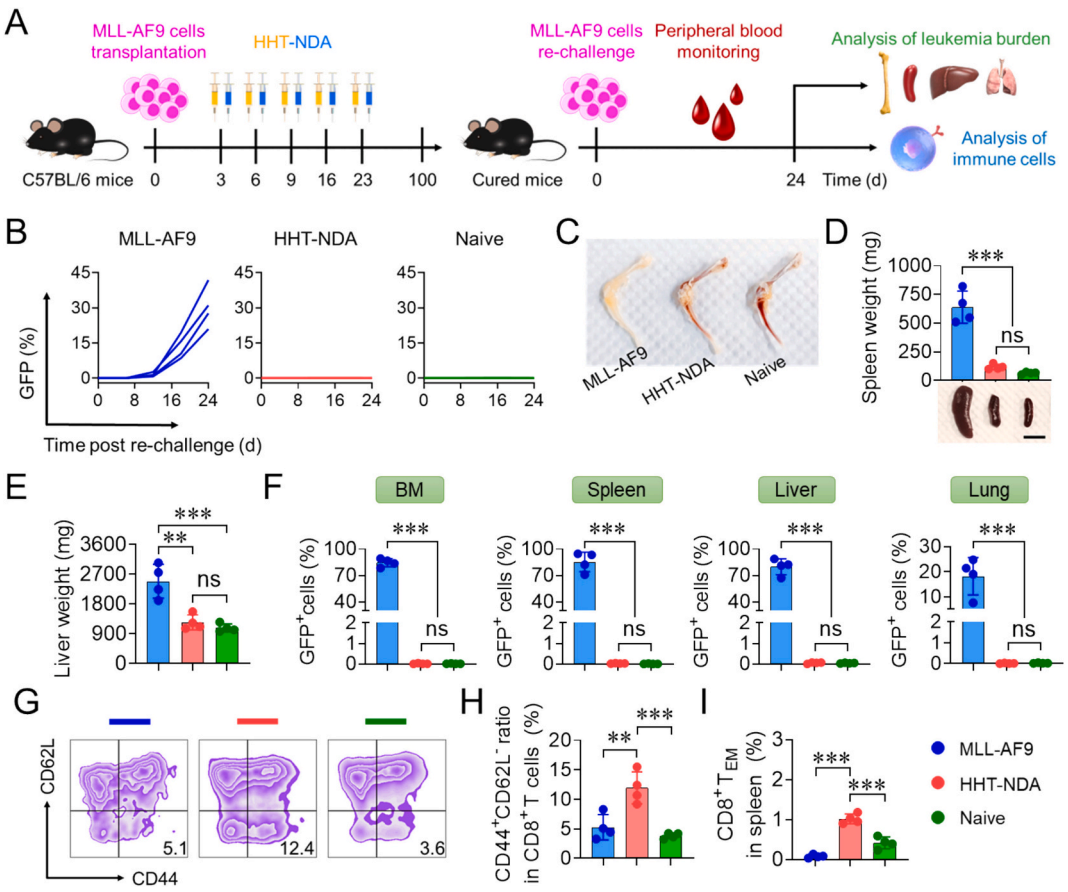

Fig. 5. HHT-NDA induced effective and long-lasting immune memory to prevent AML recurrence. (A) Timeline for the rechallenge experiment. (B) Percentage of GFP^+ AML cells progression in PB post re-challenge. (C) Phenotype of bones, (D) weight/size of spleens (scale bar: 1 cm) and (E) weight of livers from mice in different groups on day 24 post re-challenge. (F) Percentage of GFP^+ AML cells in BM, spleen, liver and lung on day 24 post re-challenge. (G) Representative flow cytometry plots and (H) ratio of T_{EM} ($CD44^+CD62L^-$) among $CD8^+$ T cells. (I) Calculated percentage of $CD8^+$ T_{EM} cells ($CD8^+CD44^+CD62L^-$) in splenocytes on day 24 post re-challenge. $n = 4$, one-way ANOVA was performed for statistical analysis, $^{**}p < 0.01$, $^{***}p < 0.001$, ns, not significant.

3.3. HHT-NDA therapy substantially improves treatment of MLL-AF9 model

To demonstrate the superior efficacy of HHT-NDA therapy, MLL-AF9-bearing mice received HHT (*i.p.*) followed by *i.v.* adjuvant infusion 10 h later (Fig. 4A). Two therapy experiments were conducted to evaluate the short term and long term efficacy respectively. By day 25 post MLL-AF9 transplantation, massive invasion of GFP^+ AML cells was observed in PB and major organs such as BM, spleen, liver and lungs in mice treated with saline (Fig. 4B, C). While treatment with HHT alone or in combination with adjuvants systemically reduced AML cells, HHT-NDA achieved the maximal efficacy, suppressing tumor cells to <0.6 % of total cells in examined organs and PB (Fig. 4B, C).

The long-term efficacy of *in situ* vaccines was then evaluated by monitoring the number of GFP^+ AML cells in PB during disease progression (by day 100) and the overall survival of mice (by day 110). HHT or NDA monotherapy induced modest delays in leukemia progression and all mice ultimately succumbed to AML. In contrast, HHT-NDA combination therapy profoundly suppressed AML proliferation and achieved complete remission in 57 % of leukemic mice (Fig. 4D, E). A similar enhancement in efficacy was observed when other chemotherapeutics such as cytarabine and doxorubicin were combined with adjuvants [39,48,49]. Notably, HHT-NDA also outperformed HHT plus free dual adjuvants (DA) (Fig. 4D, E), underscoring the crucial role of designed polymersome delivery system in augmenting adjuvant potency. The robust immunostimulation of NDA originates from its high stability in circulation and efficient intracellular delivery of MDP and CpG [28], which targets NOD2 in the cytosol and TLR9 in the endosomal membrane of DCs, respectively [50]. The polymersomes employed by NDA can not only facilitate the internalization of adjuvants into DCs but also promote rapid release of adjuvants inside cells [28,51]. Despite the robust and systemic stimulation of anti-AML immune responses, all therapies were well tolerated, as evidenced by the absence of overt body weight changes in any group of mice (Fig. 4F).

To assess HHT-NDA efficacy in advanced AML, therapy was initiated at later disease stages (Fig. 4G). Initiating HHT-NDA therapy on day 3 (T1) achieved a 71 % cure rate this time (Fig. 4H and Fig. S4). Delaying treatment initiation to day 6 (T2) reduced efficacy but still eradicated leukemia in 43 % of mice, which remained tumor-free for >300 days post-inoculation (Fig. 4H and Fig. S4). These results suggest that HHT-NDA is effective even in treating more advanced stages of AML.

HHT-NDA therapy achieved cure rates comparable to the highest efficacies reported for combinations of chemotherapy and immunostimulatory adjuvants, yet it required only a 2 to 20-fold lower doses of chemotherapeutics [39,48,49,52]. The superior efficacy of HHT-NDA therapy can be attributed to several factors. Firstly, HHT can generate abundant leukemia Ags *in vivo* by more effective killing of tumor cells. HHT has demonstrated improved treatment efficacy against AML, both as monotherapy and in combination with conventional chemotherapy regimens [53–55]. Consequently, a reduced dosage of HHT is sufficient to achieve similar potency.

Secondly, in HHT-NDA therapy, adjuvants were administered 10 h after each chemotherapy dose to improve the development of Ag-specific immunity. Conversely, some studies completed induction

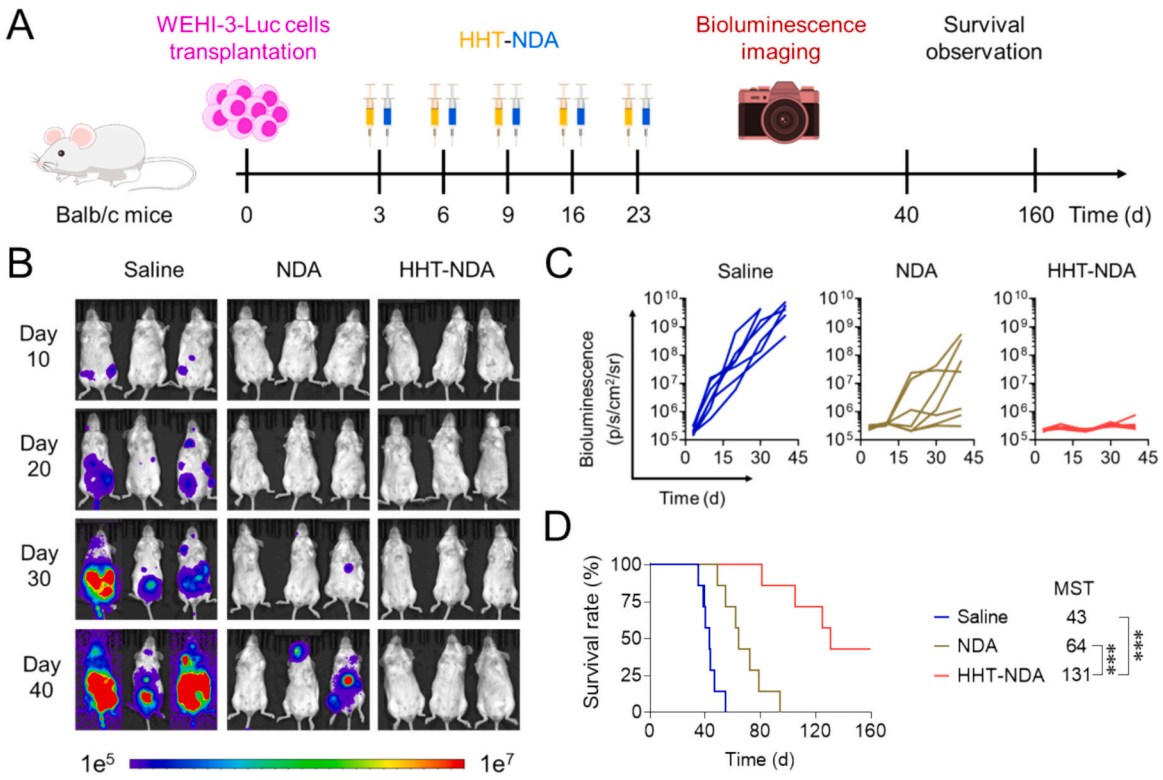

Fig. 6. HHT-NDA therapy effectively debulked WEHI-3 leukemia. (A) Timeline for the therapy experiment ($n = 7$). (B) Representative bioluminescence IVIS image and (C) bioluminescence signals of mice at different time points. (D) Survival curve. Statistical analysis was performed by log-rank test, $^{***}p < 0.001$.

chemotherapy doses before introducing immunoadjuvants, leading to suboptimal utilization of chemotherapy-induced Ags [49,52]. In cases where chemotherapy preceded adjuvant administration by weeks, it was necessary to supplement exogenously prepared Ags to effectively synergize with the adjuvants [49].

Moreover, Ags generated by chemotherapy *in vivo* proved to be more effective than those prepared exogenously. In the absence of chemotherapeutics, treatments utilizing cryoshocked leukemia cells with adjuvant MPLA or leukemia cell membranes supported by STING agonist demonstrated limited anti-AML efficacy. However, co-administration of doxorubicin (Dox) with these platforms significantly enhanced therapeutic outcomes [39,48]. As Dox typically displayed weak efficacy in murine AML models, the enhanced efficacy was likely attributable to the induced Ag-specific immune responses.

3.4. HHT-NDA therapy elicits effective and durable anti-AML immune memory

Beyond direct leukemic cell eradication, HHT-NDA therapy also established durable immunological memory to prevent AML relapse. Mice cured by HHT-NDA treatment (HHT-NDA group) were rechallenged with MLL-AF9 cells at day 77 after the last dosing, while untreated healthy mice were inoculated with the same quantity of leukemia cells (MLL-AF9 group) to serve as controls (Fig. 5A). In the MLL-AF9 group, rapid proliferation of AML cells was observed in PB, and by day 24, these mice exhibited pale (as opposed to the normal dark red) bones, swollen spleens and enlarged livers due to the extensive AML cell infiltration (Fig. 5B-F, and Fig. S5). On the contrary, the anti-AML immune memory elicited by HHT-NDA therapy effectively prevented the outgrowth of rechallenged leukemia cells in PB and major organs in 100 % of mice (Fig. 5B, F, and Fig. S5), maintaining organ phenotypes similar to those of naive healthy mice (Fig. 5C-E). Additionally, HHT-NDA treatment led to a 2.3-fold increase in the percentage of effector memory T cells (T_{EM}, $CD44^{+}CD62L^{-}$) among $CD8^{+}$ T cells and a 11.8-fold increase in the proportion of $CD8^{+}$ T_{EM} cells in splenocytes compared to that from the MLL-AF9 group (Fig. 5G-I). These findings indicate that HHT-NDA therapy can induce effective and durable immune memory to safeguard cured mice from disease relapse.

3.5. HHT-NDA therapy demonstrates broad applicability in diverse leukemia models

The therapeutic efficacy of HHT-NDA was further validated in the WEHI-3 orthotopic AML model (Fig. 6A). Saline or NDA monotherapy groups exhibited rapid leukemia progression, bioluminescence from WEHI-3-Luc cells increased rapidly, leading to death from leukemia in all cases (Fig. 6B-D). HHT-NDA therapy effectively reduced bioluminescence signals, doubling the MST compared to NDA monotherapy and achieving durable complete responses in 43 % of mice over 160 days (Fig. 6B-D). These findings demonstrate HHT-NDA's broad efficacy across AML subtypes in various murine models.

To further enhance treatment outcomes, HHT can be combined with conventional chemotherapies such as cytarabine and doxorubicin to generate a broader spectrum of Ags [54–56]. Additionally, prior to HHT-NDA therapy, it might be beneficial to apply targeted therapies, including CD123/CD33-targeted antibodies (Abs) or chimeric antigen receptor T cell (CAR-T) therapies, to selectively eliminate subsets of AML cells, thus providing complementary sources of Ags [27,57,58]. Moreover, immune checkpoint inhibitors (ICIs), such as Abs against PD-1 and PD-L1, have been used to augment the efficacy of anti-AML chemo-immunotherapies [59–61]. These ICIs may also boost the function of leukemia-specific T cells generated by HHT-NDA therapy, further improving the efficacy of *in situ* vaccines.

4. Conclusion

In summary, we developed HHT-NDA therapy, a potent *in situ* therapeutic vaccine targeting the highly heterogenous and aggressive AML.

HHT chemotherapy substantially reduced leukemia burden and induced ICD of AML cells, thereby enhancing the *in vivo* generation of abundant tumor Ags. NDAs co-delivering adjuvant MDP and CpG activated NOD2/TLR9 dual pathways and promoted complementary stimulation of DCs. Combinatorial HHT-NDA therapy elicited robust and durable anti-AML immunity, markedly improving treatment outcomes in multiple aggressive murine AML models. More importantly, HHT-NDA established long-term immune memory, protecting 100 % of the cured mice from disease recurrence. This study extends the concept of *in situ* vaccines-traditionally used for solid tumor treatment-to blood cancers, presenting a simple and effective strategy with broad potential for treating various blood cancers.

Author contribution

P.Z. and G.C. contributed equally to this work. Z.Z., Y.Z., P.Z., G.C. and T.L. conceived and designed the experiments. P.Z., G.C., X.Z., R.Y. and X.W performed the experiments. P.Z. and T.W. analyzed and processed the data. Y.Z. and P.Z. wrote the initial manuscript. P.Z., Y.Z., Z.Z. and T.L. further revised the manuscript. All authors reviewed and commented the manuscript.

Declaration of competing interest

The authors declare no conflict of interest.

Acknowledgements

This work was financially supported by National Natural Science Foundation of China (52233007), the National Key Research and Development Program of China (2021YFB3800900), "Open Competition to Select the Best Candidates" Key Technology Program for Cell Therapy of NCTIB (NCTIB2023XB02012), Interdisciplinary Basic Frontier Innovation Program of Suzhou Medical College of Soochow University (YXY2301005), Suzhou International Joint Laboratory for Diagnosis and Treatment of Brain Diseases, and Priority Academic Program Development (PAPD) of Jiangsu Higher Education Institutions.

Appendix A. Supplementary data

Supplementary data to this article can be found online at https://doi.org/10.1016/j.jconrel.2025.113851.

Data availability

The data that support the findings of this study are available from the corresponding author upon reasonable request.

References

[1] L.A. Rojas, Z. Sethna, K.C. Soares, C. Olcese, N. Pang, E. Patterson, J. Lihm, N. Ceglia, P. Guasp, A. Chu, R. Yu, A.K. Chandra, T. Waters, J. Ruan, M. Amisaki, A. Zebboudj, Z. Odgerel, G. Payne, E. Derhovanessian, F. Müller, I. Rhee, M. Yadav, A. Dobrin, M. Sadelain, M. Łuksza, N. Cohen, L. Tang, O. Basturk, M. Gönen, S. Katz, R.K. Do, A.S. Epstein, P. Momtaz, W. Park, R. Sugarman, A.M. Varghese, E. Won, A. Desai, A.C. Wei, M.I. D'Angelica, T.P. Kingham, I. Mellman, T. Merghoub, J.D. Wolchok, U. Sahin, Ö. Türeci, B.D. Greenbaum, W.R. Jarnagin, J. Drebin, E.M. O'Reilly, V.P. Balachandran, Personalized RNA neoantigen vaccines stimulate T cells in pancreatic cancer, Nature 618 (2023) 144–150, https://doi.org/10.1038/s41586-023-06063-y.

[2] C.D. Palmer, A.R. Rappaport, M.J. Davis, M.G. Hart, C.D. Scallan, S.-J. Hong, L. Gitlin, L.D. Kraemer, S. Kounlavouth, A. Yang, L. Smith, D. Schenk, M. Skoberne, K. Taquechel, M. Marrali, J.R. Jaroslavsky, C.N. Nganje, E. Maloney, R. Zhou, D. Navarro-Gomez, A.C. Greene, G. Grotenbreg, R. Greer, W. Blair, M.D. Cao, S. Chan, K. Bae, A.I. Spira, S. Roychowdhury, D.P. Carbone, B.S. Henick, C. G. Drake, B.J. Solomon, D.H. Ahn, A. Mahipal, S.B. Maron, B. Johnson, R. Rousseau, R. Yelensky, C.-Y. Liao, D.V.T. Catenacci, A. Allen, A.R. Ferguson, K. Jooss, Individualized, heterologous chimpanzee adenovirus and self-amplifying mRNA neoantigen vaccine for advanced metastatic solid tumors: phase 1 trial interim results, Nat. Med. 28 (2022) 1619–1629, https://doi.org/10.1038/s41591-022-01937-6.

[3] U. Sahin, P. Oehm, E. Derhovanessian, R.A. Jabulowsky, M. Vormehr, M. Gold, D. Maurus, D. Schwarck-Kokarakis, A.N. Kuhn, T. Omokoko, L.M. Kranz, M. Diken, S. Kreiter, H. Haas, S. Attig, R. Rae, K. Cuk, A. Kemmer-Brück, A. Breitkreuz, C. Tolliver, J. Caspar, J. Quinkhardt, L. Hebich, M. Stein, A. Hohberger, I. Vogler, I. Liebig, S. Renken, J. Sikorski, M. Leierer, V. Müller, H. Mitzel-Rink, M. Miederer, C. Huber, S. Grabbe, J. Utikal, A. Pinter, R. Kaufmann, J.C. Hassel, C. Loquai, Ö. Türeci, An RNA vaccine drives immunity in checkpoint-inhibitor-treated melanoma, Nature 585 (2020) 107–112, https://doi.org/10.1038/s41586-020-2537-9.

[4] M. Saxena, S.H. van der Burg, C.J.M. Melief, N. Bhardwaj, Therapeutic cancer vaccines, Nat. Rev. Cancer 21 (2021) 360–378, https://doi.org/10.1038/s41568-021-00346-0.

[5] E. Blass, P.A. Ott, Advances in the development of personalized neoantigen-based therapeutic cancer vaccines, Nat. Rev. Clin. Oncol. 18 (2021) 215–229, https://doi.org/10.1038/s41571-020-00460-2.

[6] P.D. Katsikis, K.J. Ishii, C. Schliehe, Challenges in developing personalized neoantigen cancer vaccines, Nat. Rev. Immunol. 24 (2024) 213–227, https://doi.org/10.1038/s41577-023-00937-y.

[7] Y. Bo, H. Wang, Biomaterial-based in situ cancer vaccines, Adv. Mater. 36 (2024) 2210452, https://doi.org/10.1002/adma.202210452.

[8] L. Diao, M. Liu, Rethinking antigen source: cancer vaccines based on whole tumor cell/tissue lysate or whole tumor cell, Adv. Sci. 10 (2023) 2300121, https://doi.org/10.1002/advs.202300121.

[9] Y. Zheng, Z. Zhong, Roadmap to next-generation cancer vaccines, J. Control. Release 347 (2022) 308–313, https://doi.org/10.1016/j.jconrel.2022.05.005.

[10] Z. Meng, Y. Zhang, X. Zhou, J. Ji, Z. Liu, Nanovaccines with cell-derived components for cancer immunotherapy, Adv. Drug Deliv. Rev. 182 (2022) 114107, https://doi.org/10.1016/j.addr.2021.114107.

[11] X. Zhang, H. Cui, W. Zhang, Z. Li, J. Gao, Engineered tumor cell-derived vaccines against cancer: the art of combating poison with poison, Bioact. Mater. 22 (2023) 491–517, https://doi.org/10.1016/j.bioactmat.2022.10.016.

[12] N. Gong, M.-G. Alameh, R. El-Mayta, L. Xue, D. Weissman, M.J. Mitchell, Enhancing in situ cancer vaccines using delivery technologies, Nat. Rev. Drug Discov. 23 (2024) 607–625, https://doi.org/10.1038/s41573-024-00974-9.

[13] Y. Chao, C. Liang, H. Tao, Y. Du, D. Wu, Z. Dong, Q. Jin, G. Chen, J. Xu, Z. Xiao, Q. Chen, C. Wang, J. Chen, Z. Liu, Localized cocktail chemoimmunotherapy after in situ gelation to trigger robust systemic antitumor immune responses, Sci. Adv. 6 (2020) eaaz4204, https://doi.org/10.1126/sciadv.aaz4204.

[14] Z. Huang, S. Huang, S. Song, Y. Ding, H. Zhou, S. Zhang, L. Weng, Y. Zhang, Y. Hu, A. Yuan, Y. Dai, Z. Luo, L. Wang, Two-dimensional coordination risedronate-manganese nanobelts as adjuvant for cancer radiotherapy and immunotherapy, Nat. Commun. 15 (2024) 8692, https://doi.org/10.1038/s41467-024-53084-w.

[15] Y. Huang, Z. Guan, X. Dai, Y. Shen, Q. Wei, L. Ren, J. Jiang, Z. Xiao, Y. Jiang, D. Liu, Z. Huang, X. Xu, Y. Luo, C. Zhao, Engineered macrophages as near-infrared light activated drug vectors for chemo-photodynamic therapy of primary and bone metastatic breast cancer, Nat. Commun. 12 (2021) 4310, https://doi.org/10.1038/s41467-021-24564-0.

[16] X. Kang, Y. Zhang, J. Song, L. Wang, W. Li, J. Qi, B.Z. Tang, A photo-triggered self-accelerated nanoplatform for multifunctional image-guided combination cancer immunotherapy, Nat. Commun. 14 (2023) 5216, https://doi.org/10.1038/s41467-023-40996-2.

[17] N. Feng, Z. Peng, X. Zhang, Y. Lin, L. Hu, L. Zheng, B.Z. Tang, J. Zhang, Strategically engineered Au(I) complexes for orchestrated tumor eradication via chemo-phototherapy and induced immunogenic cell death, Nat. Commun. 15 (2024) 8187, https://doi.org/10.1038/s41467-024-52458-4.

[18] Y. Jiang, J. Huang, C. Xu, K. Pu, Activatable polymer nanoagonist for second near-infrared photothermal immunotherapy of cancer, Nat. Commun. 12 (2021) 742, https://doi.org/10.1038/s41467-021-21047-0.

[19] Y. Guo, S.-Z. Wang, X. Zhang, H.-R. Jia, Y.-X. Zhu, X. Zhang, G. Gao, Y.-W. Jiang, C. Li, X. Chen, S.-Y. Wu, Y. Liu, F.-G. Wu, In situ generation of micrometer-sized tumor cell-derived vesicles as autologous cancer vaccines for boosting systemic immune responses, Nat. Commun. 13 (2022) 6534, https://doi.org/10.1038/s41467-022-33831-7.

[20] R. Mezzapelle, M.E. Bianchi, M.P. Crippa, Immunogenic cell death and immunogenic surrender: related but distinct mechanisms of immune surveillance, Cell Death Dis. 12 (2021) 869, https://doi.org/10.1038/s41419-021-04178-6.

[21] L. Galluzzi, E. Guilbaud, D. Schmidt, G. Kroemer, F.M. Marincola, Targeting immunogenic cell stress and death for cancer therapy, Nat. Rev. Drug Discov. 23 (2024) 445–460, https://doi.org/10.1038/s41573-024-00920-9.

[22] C. Zhao, C. Wang, W. Shan, Z. Wang, X. Chen, H. Deng, Nanomedicines for an enhanced immunogenic cell death-based in situ Cancer vaccination response, Acc. Chem. Res. 57 (2024) 905–918, https://doi.org/10.1021/acs.accounts.3c00771.

[23] T. Zhao, Y. Cai, Y. Jiang, X. He, Y. Wei, Y. Yu, X. Tian, Vaccine adjuvants: mechanisms and platforms, Signal Transduct. Target. Ther. 8 (2023) 283, https://doi.org/10.1038/s41392-023-01557-7.

[24] A.G.X. Zeng, S. Bansal, L. Jin, A. Mitchell, W.C. Chen, H.A. Abbas, M. Chan-Seng-Yue, V. Voisin, P. van Galen, A. Tierens, M. Cheok, C. Preudhomme, H. Dombret, N. Daver, P.A. Futreal, M.D. Minden, J.A. Kennedy, J.C.Y. Wang, J.E. Dick, A cellular hierarchy framework for understanding heterogeneity and predicting drug response in acute myeloid leukemia, Nat. Med. 28 (2022) 1212–1223, https://doi.org/10.1038/s41591-022-01819-x.

[25] A.E. Whiteley, T.T. Price, G. Cantelli, D.A. Sipkins, Leukaemia: a model metastatic disease, Nat. Rev. Cancer 21 (2021) 461–475, https://doi.org/10.1038/s41568-021-00355-z.

[26] K.D. Miller, L. Nogueira, A.B. Mariotto, J.H. Rowland, K.R. Yabroff, C.M. Alfano, A. Jemal, J.L. Kramer, R.L. Siegel, Cancer treatment and survivorship statistics, CA Cancer J. Clin. 69 (2019) (2019) 363–385, https://doi.org/10.3322/caac.21565.
[27] N. Daver, A.S. Alotaibi, V. Bücklein, M. Subklewe, T-cell-based immunotherapy of acute myeloid leukemia: current concepts and future developments, Leukemia 35 (2021) 1843–1863, https://doi.org/10.1038/s41375-021-01253-x.
[28] P. Zhang, T. Wang, G. Cui, R. Ye, W. Wan, T. Liu, Y. Zheng, Z. Zhong, Systemic multifunctional Nanovaccines for potent personalized immunotherapy of acute myeloid leukemia, Adv. Mater. 36 (2024) 2407189, https://doi.org/10.1002/adma.202407189.
[29] C. Li, L. Dong, R. Su, Y. Bi, Y. Qing, X. Deng, Y. Zhou, C. Hu, M. Yu, H. Huang, X. Jiang, X. Li, X. He, D. Zou, C. Shen, L. Han, M. Sun, J. Skibbe, K. Ferchen, X. Qin, H. Weng, H. Huang, C. Song, J. Chen, J. Jin, Homoharringtonine exhibits potent anti-tumor effect and modulates DNA epigenome in acute myeloid leukemia by targeting SP1/TET1/5hmC, Haematologica 105 (2020) 148–160, https://doi.org/10.3324/haematol.2018.208835.
[30] B. Wang, X. Wen, R. Zhang, G. Zhu, Y. Wu, Y. Zhang, W. Lin, J. Yu, J. Fan, J. Li, J. Yang, M. Qin, H. Zheng, Homoharringtonine-based induction therapy reduces the recurrence rate of pediatric acute myeloid leukemia after allogeneic hematopoietic stem cell transplantation, Cell Transplant. 32 (2023), https://doi.org/10.1177/09636897231183559, 09636897231183559.
[31] A. Quintás-Cardama, H. Kantarjian, J. Cortes, Homoharringtonine, omacetaxine mepesuccinate, and chronic myeloid leukemia circa 2009, Cancer 115 (2009) 5382–5393, https://doi.org/10.1002/cncr.24601.
[32] S. Lü, J. Wang, Homoharringtonine and omacetaxine for myeloid hematological malignancies, J. Hematol. Oncol. 7 (2014) 2, https://doi.org/10.1186/1756-8722-7-2.
[33] S.K. Bohlander, A new kid on the block for acute myeloid leukemia treatment? Homoharringtonine interferes with key pathways in acute myeloid leukemia cells, Haematologica 105 (2020) 7–9, https://doi.org/10.3324/haematol.2019.234880.
[34] S.S.Y. Lam, E.S.K. Ho, B.-L. He, W.-W. Wong, C.-Y. Cher, N.K.L. Ng, C.-H. Man, H. Gill, A.M.S. Cheung, H.-W. Ip, C.-C. So, J. Tamburini, C.W.E. So, D.N. Ho, C.-H. Au, T.-L. Chan, E.S.K. Ma, R. Liang, Y.-L. Kwong, A.Y.H. Leung, Homoharringtonine (omacetaxine mepesuccinate) as an adjunct for FLT3-ITD acute myeloid leukemia, Sci. Transl. Med. 8 (2016) 359ra129, https://doi.org/10.1126/scitranslmed.aaf3735.
[35] X.-J. Chen, W.-N. Zhang, B. Chen, W.-D. Xi, Y. Lu, J.-Y. Huang, Y.-Y. Wang, J. Long, S.-F. Wu, Y.-X. Zhang, S. Wang, S.-X. Li, T. Yin, M. Lu, X.-D. Xi, J.-M. Li, K.-K. Wang, Z. Chen, S.-J. Chen, Homoharringtonine deregulates MYC transcriptional expression by directly binding NF-κB repressing factor, Proc. Natl. Acad. Sci. 116 (2019) 2220–2225, https://doi.org/10.1073/pnas.1818539116.
[36] C.P. Mill, W. Fiskus, C.D. DiNardo, C. Birdwell, J.A. Davis, T.M. Kadia, K. Takahashi, N. Short, N. Daver, M. Ohanian, G. Borthakur, S.M. Kornblau, M. R. Green, Y. Qi, X. Su, J.D. Khoury, K.N. Bhalla, Effective therapy for AML with RUNX1 mutation by cotreatment with inhibitors of protein translation and BCL2, Blood 139 (2022) 907–921, https://doi.org/10.1182/blood.2021013156.
[37] G. Cui, Y. Sun, S. Wang, F. Meng, Z. Zhong, Muramyl dipeptide-presenting Polymersomes as artificial Nanobacteria to boost systemic antitumor immunity, ACS Appl. Mater. Interfaces 16 (2024), https://doi.org/10.1021/acsami.4c13041.
[38] Y. Wang, Z. Wang, B. Chen, Q. Yin, M. Pan, H. Xia, B. Zhang, Y. Yan, Z. Jiang, Q. Zhang, Y. Wang, Cooperative self-assembled nanoparticle induces sequential immunogenic cell death and toll-like receptor activation for synergistic chemo-immunotherapy, Nano Lett. 21 (2021) 4371–4380, https://doi.org/10.1021/acs.nanolett.1c00977.
[39] T. Ci, H. Li, G. Chen, Z. Wang, J. Wang, P. Abdou, Y. Tu, G. Dotti, Z. Gu, Cryo-shocked cancer cells for targeted drug delivery and vaccination, Sci. Adv. 6 (2020) eabc3013, https://doi.org/10.1126/sciadv.abc3013.
[40] C.A. Thaiss, M. Levy, S. Itav, E. Elinav, Integration of innate immune signaling, Trends Immunol. 37 (2016) 84–101, https://doi.org/10.1016/j.it.2015.12.003.
[41] Z. Li, X. Lai, S. Fu, L. Ren, H. Cai, H. Zhang, Z. Gu, X. Ma, K. Luo, Immunogenic cell death activates the tumor immune microenvironment to boost the immunotherapy efficiency, Adv. Sci. 9 (2022) 2201734, https://doi.org/10.1002/advs.202201734.
[42] F. Yuan, D. Li, G. Li, C. Cheng, X. Wei, Synergistic efficacy of homoharringtonine and venetoclax on acute myeloid leukemia cells and the underlying mechanisms, Ann. Transl. Med. 10 (2022) 490, https://doi.org/10.21037/atm-22-1459.
[43] M.S. Shafat, T. Oellerich, S. Mohr, S.D. Robinson, D.R. Edwards, C.R. Marlein, R. E. Piddock, M. Fenech, L. Zaitseva, A. Abdul-Aziz, J. Turner, J.A. Watkins, M. Lawes, K.M. Bowles, S.A. Rushworth, Leukemic blasts program bone marrow adipocytes to generate a protumoral microenvironment, Blood 129 (2017) 1320–1332, https://doi.org/10.1182/blood-2016-08-734798.
[44] K. Melgar, M.M. Walker, L.M. Jones, L.C. Bolanos, K. Hueneman, M. Wunderlich, J.-K. Jiang, K.M. Wilson, X. Zhang, P. Sutter, A. Wang, X. Xu, K. Choi, G. Tawa, D. Lorimer, J. Abendroth, E. O'Brien, S.B. Hoyt, E. Berman, C.A. Famulare, J. C. Mulloy, R.L. Levine, J.P. Perentesis, C.J. Thomas, D.T. Starczynowski, Overcoming adaptive therapy resistance in AML by targeting immune response pathways, Sci. Transl. Med. 11 (2019) eaaw8828, https://doi.org/10.1126/scitranslmed.aaw8828.
[45] P. Williams, S. Basu, G. Garcia-Manero, C.S. Hourigan, K.A. Oetjen, J.E. Cortes, F. Ravandi, E.J. Jabbour, Z. Al-Hamal, M. Konopleva, J. Ning, L. Xiao, J. Hidalgo Lopez, S.M. Kornblau, M. Andreeff, W. Flores, C. Bueso-Ramos, J. Blando, P. Galera, K.R. Calvo, G. Al-Atrash, J.P. Allison, H.M. Kantarjian, P. Sharma, N. G. Daver, The distribution of T-cell subsets and the expression of immune checkpoint receptors and ligands in patients with newly diagnosed and relapsed acute myeloid leukemia, Cancer 125 (2019) 1470–1481, https://doi.org/10.1002/cncr.31896.
[46] R. Wang, W. Feng, H. Wang, L. Wang, X. Yang, F. Yang, Y. Zhang, X. Liu, D. Zhang, Q. Ren, X. Feng, G. Zheng, Blocking migration of regulatory T cells to leukemic hematopoietic microenvironment delays disease progression in mouse leukemia model, Cancer Lett. 469 (2020) 151–161, https://doi.org/10.1016/j.canlet.2019.10.032.
[47] D.M. Klinman, Immunotherapeutic uses of CpG oligodeoxynucleotides, Nat. Rev. Immunol. 4 (2004) 249–259, https://doi.org/10.1038/nri1329.
[48] X. Wang, R. Huang, W. Wu, J. Xiong, Q. Wen, Y. Zeng, T. Chen, J. Li, C. Zhang, J. F. Zhong, S. Yang, X. Zhang, Amplifying STING activation by bioinspired nanomedicine for targeted chemo- and immunotherapy of acute myeloid leukemia, Acta Biomater. 157 (2023) 381–394, https://doi.org/10.1016/j.actbio.2022.11.007.
[49] D.T. Johnson, J. Zhou, A.V. Kroll, R.H. Fang, M. Yan, C. Xiao, X. Chen, J. Kline, L. Zhang, D.-E. Zhang, Acute myeloid leukemia cell membrane-coated nanoparticles for cancer vaccination immunotherapy, Leukemia 36 (2022) 994–1005, https://doi.org/10.1038/s41375-021-01432-w.
[50] T. Shekarian, S. Valsesia-Wittmann, J. Brody, M.C. Michallet, S. Depil, C. Caux, A. Marabelle, Pattern recognition receptors: immune targets to enhance cancer immunotherapy, Ann. Oncol. 28 (2017) 1756–1766, https://doi.org/10.1093/annonc/mdx179.
[51] G. Cui, Y. Sun, L. Qu, C. Shen, Y. Sun, F. Meng, Y. Zheng, Z. Zhong, Uplifting antitumor immunotherapy with lymph-node-targeted and ratio-controlled Codelivery of tumor cell lysate and adjuvant, Adv. Healthc. Mater. 13 (2024) 2303690, https://doi.org/10.1002/adhm.202303690.
[52] N.J. Shah, A.J. Najibi, T.-Y. Shih, A.S. Mao, A. Sharda, D.T. Scadden, D.J. Mooney, A biomaterial-based vaccine eliciting durable tumour-specific responses against acute myeloid leukaemia, Nat. Biomed. Eng. 4 (2020) 40–51, https://doi.org/10.1038/s41551-019-0503-3.
[53] J. Jin, D.Z. Jiang, W.Y. Mai, H.T. Meng, W.B. Qian, H.Y. Tong, J. Huang, L.P. Mao, Y. Tong, L. Wang, Z.M. Chen, W.L. Xu, Homoharringtonine in combination with cytarabine and aclarubicin resulted in high complete remission rate after the first induction therapy in patients with de novo acute myeloid leukemia, Leukemia 20 (2006) 1361–1367, https://doi.org/10.1038/sj.leu.2404287.
[54] Y. Ma, X. Zhang, J. Hou, L. Shen, F. Li, F. Kong, Y. Lu, G. Li, J. Jin, W. Yu, Azacitidine, Homoharringtonine and Cytarabine combined with granulocyte Colony-stimulating factor as frontline treatment for older patients with acute myeloid leukemia: a prospective, multicenter, single-arm phase III study in China, Blood 144 (2024) 4280, https://doi.org/10.1182/blood-2024-203359.
[55] D. Yan, H. Wei, X. Lai, Y. Ge, S. Xu, J. Meng, T. Wen, J. Liu, W. Zhang, J. Wang, H. Xu, Co-delivery of homoharringtonine and doxorubicin boosts therapeutic efficacy of refractory acute myeloid leukemia, J. Control. Release 327 (2020) 766–778, https://doi.org/10.1016/j.jconrel.2020.09.031.
[56] J. Jin, J.-X. Wang, F.-F. Chen, D.-P. Wu, J. Hu, J.-F. Zhou, J.-D. Hu, J.-M. Wang, J.-Y. Li, X.-J. Huang, J. Ma, C.-Y. Ji, X.-P. Xu, K. Yu, H.-Y. Ren, Y.-H. Zhou, Y. Tong, Y.-J. Lou, W.-M. Ni, H.-Y. Tong, H.-F. Wang, Y.-C. Mi, X. Du, B.-A. Chen, Y. Shen, Z. Chen, S.-J. Chen, Homoharringtonine-based induction regimens for patients with de-novo acute myeloid leukaemia: a multicentre, open-label, randomised, controlled phase 3 trial, Lancet Oncol. 14 (2013) 599–608, https://doi.org/10.1016/S1470-2045(13)70152-9.
[57] K. Knorr, J. Rahman, C. Erickson, E. Wang, M. Monetti, Z. Li, J. Ortiz-Pacheco, A. Jones, S.X. Lu, R.F. Stanley, M. Baez, N. Fox, C. Castro, A.E. Marino, C. Jiang, A. Penson, S.J. Hogg, X. Mi, H. Nakajima, H. Kunimoto, K. Nishimura, D. Inoue, B. Greenbaum, D. Knorr, J. Ravetch, O. Abdel-Wahab, Systematic evaluation of AML-associated antigens identifies anti-U5 SNRNP200 therapeutic antibodies for the treatment of acute myeloid leukemia, Nat. Can. 4 (2023) 1675–1692, https://doi.org/10.1038/s43018-023-00656-2.
[58] A.S. Bhagwat, L. Torres, O. Shestova, M. Shestov, P.W. Mellors, H.R. Fisher, S. N. Farooki, B.F. Frost, M.R. Loken, A.L. Gaymon, D. Frazee, W. Rogal, N. Frey, E. O. Hexner, S.M. Luger, A.W. Loren, M.E. Martin, S.R. McCurdy, A.E. Perl, E. A. Stadtmauer, J.L. Brogdon, J.A. Fraietta, W.-T. Hwang, D.L. Siegel, G. Plesa, R. Aplenc, D.L. Porter, C.H. June, S.I. Gill, Cytokine-mediated CAR T therapy resistance in AML, Nat. Med. (2024), https://doi.org/10.1038/s41591-024-03271-5.
[59] M. Chen, Y. Qiao, J. Cao, L. Ta, T. Ci, X. Ke, Biomimetic doxorubicin/ginsenoside co-loading nanosystem for chemoimmunotherapy of acute myeloid leukemia, J. Nanobiotechnol. 20 (2022) 273, https://doi.org/10.1186/s12951-022-01491-w.
[60] A.R. Shin, S.-E. Lee, H. Choi, H.-J. Sohn, H.-I. Cho, T.-G. Kim, An effective peptide vaccine strategy circumventing clonal MHC heterogeneity of murine myeloid leukaemia, Br. J. Cancer 123 (2020) 919–931, https://doi.org/10.1038/s41416-020-0955-y.
[61] X. Xie, Y. Hu, T. Ye, Y. Chen, L. Zhou, F. Li, X. Xi, S. Wang, Y. He, X. Gao, W. Wei, G. Ma, Y. Li, Therapeutic vaccination against leukaemia via the sustained release of co-encapsulated anti-PD-1 and a leukaemia-associated antigen, Nat. Biomed. Eng. 5 (2021) 414–428, https://doi.org/10.1038/s41551-020-00624-6.